Molecular Pharmacology Fast Forward. Published on April 26, 2011 as DOI: 10.1124/mol.111.072413
This article has not been copyedited and formatted. The final version may differ from this version.
Molecular Pharmacology Fast Forward. Published on April 26, 2011 as doi:10.1124/mol.111.072413

Title Page

Substrate specificity and ligand interactions of CYP26A1, the human liver retinoic acid hydroxylase

Jayne E. Thatcher, Brian Buttrick, Scott A. Shaffer, Jakob A. Shimshoni, David R. Goodlett, Wendel L. Nelson, Nina Isoherranen

Department of Pharmaceutics (JET, BB, JAS, NI) and Department of Medicinal Chemistry (SAS, DRG, WLN), School of Pharmacy, University of Washington, Seattle, Washington;

Downloaded from molpharm.aspetjournals.org at ASPET Journals on April 16, 2024

Copyright 2011 by the American Society for Pharmacology and Experimental Therapeutics.

Molecular Pharmacology Fast Forward. Published on April 26, 2011 as DOI: 10.1124/mol.111.072413
This article has not been copyedited and formatted. The final version may differ from this version.

Running title page:

Running title: Interaction of xenobiotic ligands with CYP26A1

Corresponding Author:

Nina Isoherranen, Department of Pharmaceutics, Box 357610, University of Washington, Seattle, WA 98195. Phone: (206) 543-2517 Fax: (206) 543-3204 E-mail: ni2@u.washington.edu

Number of text pages 23

Number of tables: 2

Number of figures: 7

Number of references: 40

Number of words in:

Abstract: 249

Introduction: 654

Discussion: 1483

Nonstandard abbreviations used:

IC_{50} – Concentration at which 50% of the enzyme activity is inhibited

RAMBA – Retinoic acid metabolism blocking agent

*at*RA – all trans retinoic acid

Downloaded from molpharm.aspetjournals.org at ASPET Journals on April 16, 2024

Molecular Pharmacology Fast Forward. Published on April 26, 2011 as DOI: 10.1124/mol.111.072413
This article has not been copyedited and formatted. The final version may differ from this version.

9-*cis*RA – 9-cis retinoic acid

13-*cis*RA – 13-cis retinoic acid

HPLC – high performance liquid chromatography

LTQ – linear ion trap

UPLC – ultra high performance liquid chromatography

MS – mass spectrometry

rt – retention time

RAR – retinoic acid receptor

RXR – retinoid X receptor

PPAR – peroxisome proliferator-activated receptor

KPi – phosphate buffer

R115866 – (R)-N-[4-[2-ethyl-1-(1*H*-1,2,4-triazol-1-yl)butyl]phenyl]-2-benzothiazolamine

R116010 – [S-(R*,R*)]-N-[4-[2-(dimethylamino)-1-(1*H*-imidazole-1-yl)propyl]-phenyl]-2-benzothiazolamine

CS5 – 2-[1-(4-hydroxyphenyl)methylidene]-3,4-dihydro-2*H*-napthalen-1-one

CS6 – 2-4(-hydroxybenzyl)-6-methoxy-3,4-dihydro-2*H*-napthalen-1-one

CD 1530 4-(6-hydroxy-7-tricyclo[3.3.1.13,7]dec-1-yl-2-naphthalenyl)benzoic acid

Downloaded from molpharm.aspetjournals.org at ASPET Journals on April 16, 2024

Molecular Pharmacology Fast Forward. Published on April 26, 2011 as DOI: 10.1124/mol.111.072413
This article has not been copyedited and formatted. The final version may differ from this version.

TTNPB - 4-[(E)-2-(5,6,7,8-tetrahydro-5,5,8,8-tetramethyl-2-naphthalenyl)-1-propenyl]benzoic acid

L-165,041 - [4-[3-(4-acetyl-3-hydroxy-2-propylphenoxy)propoxy]phenoxy]acetic acid

AM 580 - 4-[(5,6,7,8-tetrahydro-5,5,8,8-tetramethyl-2-naphthalenyl)carboxamido]benzoic acid

GW 9662 - 2-chloro-5-nitro-N-phenylbenzamide

AC 55649 - 4'-octyl-[1,1'-biphenyl]-4-carboxylic acid

Downloaded from molpharm.aspetjournals.org at ASPET Journals on April 16, 2024

Molecular Pharmacology Fast Forward. Published on April 26, 2011 as DOI: 10.1124/mol.111.072413
This article has not been copyedited and formatted. The final version may differ from this version.

Abstract

All-trans retinoic acid (*at*RA) is the active metabolite of vitamin A. *at*RA is also used as a drug, and synthetic *at*RA analogues and inhibitors of RA metabolism have been developed. The hepatic clearance of *at*RA is mediated primarily by CYP26A1, but design of CYP26A1 inhibitors is hindered by lack of information on CYP26A1 structure and structure activity relationships of its ligands. This study was aimed at identifying the primary metabolites of *at*RA formed by CYP26A1 and at characterizing the ligand selectivity and ligand interactions of CYP26A1. Based on high resolution MS/MS data, the four primary metabolites formed from *at*RA by CYP26A1 were identified as 4OH-RA, 4oxo-RA, 16OH-RA and 18OH-RA. 9-*cis*RA and 13-*cis*RA were also substrates of CYP26A1. Forty-two compounds with diverse structural properties were tested for CYP26A1 inhibition using 9-*cis*RA as a probe, and IC_{50} values for ten inhibitors were determined. The imidazole and triazole containing inhibitors R116010 and R115866 were the most potent inhibitors of CYP26A1 with IC_{50} values of 4.3 and 5.1nM, respectively. Liarozole and ketoconazole were significantly less potent with IC_{50} values of 2100 and 550nM, respectively. The RARγ agonist CD1530 was as potent inhibitor of CYP26A1 as ketoconazole with an IC_{50} of 530nM, whereas the tested RARα and RARβ agonists did not significantly inhibit CYP26A1. The pan-RAR agonist TTNPB and the PPAR ligands rosiglitazone and pioglitazone inhibited CYP26A1 with IC_{50} values of 3.7, 4.2 and 8.6μM respectively. These data demonstrate that CYP26A1 has high ligand selectivity but accepts structurally related nuclear receptor agonists as inhibitors.

Downloaded from molpharm.aspetjournals.org at ASPET Journals on April 16, 2024

Molecular Pharmacology Fast Forward. Published on April 26, 2011 as DOI: 10.1124/mol.111.072413
This article has not been copyedited and formatted. The final version may differ from this version.

Introduction

All-*trans* retinoic acid (*at*RA) is the biologically active metabolite of vitamin A (retinol), but three other isomers of retinoic acid (9-*cis*RA, 13-*cis*RA, and 9,13-*dicis*RA) can also be detected *in vivo* (Kane et al., 2010; Kane et al., 2008). During development atRA regulates cell differentiation (Duester, 2008), and during adult life it is important for maintaining healthy epithelia, immunity, fertility and regulating cell proliferation (Blomhoff and Blomhoff, 2006). Retinoic acid isomers also play a role in adult neurogenesis and cell survival (Jacobs et al., 2006), and they contribute to regulation of glucose homeostasis (Kane et al., 2010). The many biological effects of atRA are believed to result from atRA binding to three nuclear retinoic acid receptors (RARα, RARβ and RARγ), which are activated by RA isomers resulting in induction of gene transcription (Altucci et al., 2007; Petkovich et al., 1987; Tang and Gudas, 2011). *at*RA, 9-*cis*RA and 13-*cis*RA are all used clinically in treatment of various cancers and skin diseases but the clinical use of endogenous retinoids has been limited due to side effects caused by off-target effects and development of resistance (Altucci et al., 2007; Garattini et al., 2007).

Resistance to *at*RA treatment in cancer therapy is attributed to increased systemic clearance and cellular metabolism of *at*RA during treatment (Muindi et al., 1992; van der Leede et al., 1997). To improve therapeutic outcomes, synthetic RA analogues, RAR agonists, and RA metabolism blocking agents (RAMBAs) have been developed and tested for treatment of cancers and skin diseases (Altucci et al., 2007; Njar et al., 2006). The first tested inhibitors of *at*RA metabolism included liarozole (R75251) and ketoconazole that inhibited metabolism of *at*RA *in vivo* in rats and in *in vitro* models (Van Wauwe et al., 1990; Van Wauwe et al., 1988; Wouters et al., 1992). Subsequently, more specific and potent inhibitors of *at*RA

Downloaded from molpharm.aspetjournals.org at ASPET Journals on April 16, 2024

Molecular Pharmacology Fast Forward. Published on April 26, 2011 as DOI: 10.1124/mol.111.072413
This article has not been copyedited and formatted. The final version may differ from this version.

metabolism synthesized by several groups showed potential for treatment of cancers and skin diseases in both *in vitro* and *in vivo* models (Mulvihill et al., 2005; Njar et al., 2006; Patel et al., 2004; Yee et al., 2005).

CYP26A1 appears to be a likely target of development of new inhibitors of *at*RA metabolism. It is likely that CYP26A1, a CYP identified as a RA hydroxylase that is upregulated by *at*RA (White et al., 1996), is induced during *at*RA treatment. *at*RA has high affinity for and is efficiently metabolized by CYP26A1 (Lutz et al., 2009), and CYP26A1 is the primary enzyme responsible for hepatic clearance of *at*RA (Thatcher et al., 2010). CYP26A1 is also inducible by *at*RA in human liver (Tay et al., 2010). However, neither the structure of CYP26A1 nor the structural requirements of potent CYP26A1 binding are well characterized. Three homology models of CYP26A1 have been reported (Gomaa et al., 2006; Karlsson M, 2008; Ren et al., 2008) based on the crystal structures of CYP3A4, CYP2C8, CYP2C9 and CYP51. However, experimental data on ligand overlap, *at*RA binding orientations and metabolite identification are not available to support the construction of these models, perhaps due to a lack of a system to screen CYP26A1 ligands. Use of *at*RA as a substrate to screen CYP26A1 inhibitors is not feasible in cell systems and with recombinant CYP26A1, because the primary metabolites are rapidly depleted making measurements of catalytic activity confounding. In addition, *at*RA binds CYP26A1 with high affinity (K_m=9.3 nM) (Lutz et al., 2009) requiring very sensitive assays to measure product formation if substrate is added at the K_m or lower concentration. Therefore an alternative substrate of CYP26A1 is needed. In this study 9-*cis*RA was evaluated as an alternative substrate for inhibitor screening, the specific metabolites of *at*RA and 9-*cis*RA formed by CYP26A1 were identified, and the overall ligand selectivity of CYP26A1 was established.

Downloaded from molpharm.aspetjournals.org at ASPET Journals on April 16, 2024

Molecular Pharmacology Fast Forward. Published on April 26, 2011 as DOI: 10.1124/mol.111.072413
This article has not been copyedited and formatted. The final version may differ from this version.

The obtained data will be valuable for rationalization of observed *in vivo* interactions between xenobiotics and *at*RA, for design of new CYP26A1 inhibitors and for refining features of existing homology models of CYP26A1.

Downloaded from molpharm.aspetjournals.org at ASPET Journals on April 16, 2024

Molecular Pharmacology Fast Forward. Published on April 26, 2011 as DOI: 10.1124/mol.111.072413
This article has not been copyedited and formatted. The final version may differ from this version.

Materials and methods

Chemicals: *at*RA, 9-*cis*RA, acitretin, GW 9662, L-165,041, AM 580, ketoconazole, itraconazole, fluconazole, quinapril, propranolol, methoxypsoralen, quinidine, omeprazole, diltiazem, erythromycin, paclitaxel, pimozide, ranolazine, terfenadine, verapamil, simvastatin, danazol and NADPH were purchased from Sigma-Aldrich (St. Louis, MO). Cyclosporine and tamoxifen were purchased from Enzo Life Sciences International, Inc. (formerly BIOMOL International, L.P.) (Plymouth Meeting, PA). Voriconazole was a gift from Dr. Kenneth E. Thummel, University of Washington. CS5 and CS6 were gifts from Dr. Claire Simons (Medicinal Chemistry, Welsh School of Pharmacy, Cardiff University, Cardiff, UK). R115866 and R116010 were gifts from Johnson and Johnson, Beerse, Belgium. Liarozole, TTNPB, AC55649, and CD1530 were purchased from Tocris Biosciences (Ellisville, MO). *at*RA-d5 was purchased from Santa Cruz Biotechnology, Inc (Santa Cruz, CA). Rosiglitazone was purchased from Cayman Chemical Company (Ann Arbor, Michigan) and pioglitazone was purchased from Altan Biochemicals (Orange, CT). 3OH-retinal and 4OH-9*cis*RA was purchased from Toronto Research Chemicals (Toronto, ON). The protease inhibitors used in this study were obtained from the NIH AIDS Research and Reference Reagent Program (Germantown, MD). CYP26A1 was expressed in Sf9 cells as previously described and utilized as microsomal fractions supplemented with rat P450 reductase expressed in *E. coli* (Lutz et al., 2009). All solvents used were HPLC grade or higher and purchased from EMD Chemicals (Gibbstown, NJ), JT Baker (Phillipsburg, NJ), or Fisher Scientific (Pittsburg, PA.)

Synthesis of 3OH-atRA: 3OH-*at*RA was synthesized by oxidation of 3OH-retinal with Tollens' reagent (Barua and Barua, 1964). The Tollens' reagent was freshly prepared prior to use by

Downloaded from molpharm.aspetjournals.org at ASPET Journals on April 16, 2024

Molecular Pharmacology Fast Forward. Published on April 26, 2011 as DOI: 10.1124/mol.111.072413
This article has not been copyedited and formatted. The final version may differ from this version.

mixing equal volumes of 10% w/w $AgNO_3$ and 10% w/w NaOH. Ammonium hydroxide solution (Sigma-Aldrich) was added dropwise to dissolve the precipitated Ag_2O. Tollens' reagent (1 mL) was added slowly to 3 mg of 3OH-Retinal dissolved in 8 mL of methanol and stirred for 6 hours at 37 ºC. The reaction was quenched by acidification with aqueous 0.5 N HCl. The product was extracted with dichloromethane, dried over Na_2SO_4 and evaporated to dryness. The identity of the product was verified by NMR analysis. ^{1}H-NMR (500 MHz, $CDCl_3$) δ 0.97 (s, 3H, 16-CH_3), 0.98 (s, 3H, 17-CH_3), 1.76 (s, 3H, 18-CH_3), 2.04 (s, 3H, 19-CH_3), 2.38 (s, 3H, 20-CH_3), 4.03 (t, 1H, 3-H), 5.83 (s, 1H, 14-H), 6.09 (d, 1H, 8-H), 6.19 (d, 1H, 10-H), 6.27 (d, 1H, 12-H), 6.35 (d, 1H, 7-H), 7.05 (dd, 1H, 11-H). The product was also analyzed by HPLC-UV as described below for hydroxylated metabolites and had a retention time of 14.9 min, 0.8 min before the 4OH-RA standard that eluted at 15.7 min.

Incubation conditions and HPLC analysis for RA isomers: Unless otherwise described, incubations were performed with 5 pmol of CYP26A1 and 10 pmol of P450 reductase. The purified rat reductase was added to CYP26A1 microsomes and the reductase was allowed to incorporate into the membrane for 10 minutes at room temperature. The final volume of each incubation sample was then brought to 1 mL by adding 100 mM KPi buffer (pH 7.4), 9-*cis*RA and where appropriate, inhibitor or solvent. Compounds were dissolved in methanol or DMSO and final solvent amounts in the incubations were kept at 1%. The samples were preincubated for 5 minutes at 37 ºC before the reaction was initiated with 1 mM NADPH. Unless otherwise noted, incubation times were 1 minute. Extraction of RA and its metabolites, followed by HPLC analysis was performed as previously published (Thatcher et al., 2010). In brief, incubations were terminated with 5 mL of ethyl acetate and acitretin was added as an internal standard. The ethyl acetate layer was evaporated and reconstituted in

Downloaded from molpharm.aspetjournals.org at ASPET Journals on April 16, 2024

Molecular Pharmacology Fast Forward. Published on April 26, 2011 as DOI: 10.1124/mol.111.072413
This article has not been copyedited and formatted. The final version may differ from this version.

methanol. Analytes were separated by HPLC and detected with a multiple wavelength detector, monitoring at 360 nm. Data analysis was performed using HP Chemstation software.

Characterization of atRA and 9-cisRA metabolism by CYP26A1: To determine whether other RA isomers (9-*cis*RA and 13-*cis*RA) are substrates of CYP26A1, and to identify the metabolites formed from *at*RA and 9-*cis*RA by CYP26A1, 9-*cis*RA, *at*RA-d_5 and *at*RA were incubated at 100 μM concentration in the presence of 100 pmol CYP26A1 and 200 pmol reductase for 1 hour. The structures of these compounds are shown in Fig 1. Additionally, 9-*cis*RA, 13-*cis*RA and *at*RA were incubated at 500 nM concentration in the presence of 5 pmol CYP26A1 and 10 pmol of P450 reductase for 2 minutes. Samples were analyzed by HPLC as described above. Fractions from the incubations performed with 100 μM substrate were collected for mass spectrometric analysis. Full scan and tandem mass spectra were acquired on an LTQ-Orbitrap (Thermo Scientific, Pittsburgh, PA) hybrid mass spectrometer operated in the negative ion electrospray mode. Fractions were introduced by infusion using a NanoAcquity UPLC (Waters, Milford, MA) interfaced to a CaptiveSpray (Michrom Bioresources, Auburn, CA) ion source. Samples were injected in 10 μL and infused in 1:1 mixture of water/acetonitrile containing 0.1% formic acid (v/v) flowing at 5 μL/minute. Full scan mass spectra were acquired in the Orbitrap at 60,000 resolution. Collision induced dissociation occurred in the LTQ using a normalized collision energy of 35%, an isolation width of 4 Da, but with the resulting tandem mass spectra acquired in the Orbitrap at 15,000 resolution. Data-dependent parameters were programmed to allow a cycle of one mass spectrum followed by tandem mass spectra of the three most abundant ions. All other data-dependent parameters were minimized to allow for maximum data-redundancy (i.e. scan

Downloaded from molpharm.aspetjournals.org at ASPET Journals on April 16, 2024

Molecular Pharmacology Fast Forward. Published on April 26, 2011 as DOI: 10.1124/mol.111.072413
This article has not been copyedited and formatted. The final version may differ from this version.

averaging). Data analysis of MS/MS fragments was performed with Thermo Xcalibur software.

The metabolites of 9-*cis*RA were further characterized using an AB Sciex API5500 Q/LIT mass spectrometer equipped with an Agilent 1290 Infinity UPLC and Agilent Zorbax C18 column (3.5 mm, 2.1 x 100 mm). The metabolites were separated using gradient elution from 90 % acetonitrile and aqueous 10 % ammonium acetate (50 mM) to 90 % acetonitrile over 15 minutes. The column was maintained at 25 °C and the injection volume was 10 μL. Negative ion electrospray was used and the ion source voltage (IS) and source temperature (TEM) were set at -4500 V and 400 °C, respectively. The MRM transitions of m/z = 315 > 253 Da and m/z = 315 > 241 Da were monitored. For both transitions, the declustering potential (DP), collision energy (CE) and collision exit potential (CXP) were set to -90 V, -25 V, and -10 V, respectively. In parallel, daughter ion scans of m/z = 315 were collected from 100 to 350 *m/z*. The detection settings for the scan parameters were identical to those for MRM runs.

Determination of kinetic constants of 9-cisRA metabolism by CYP26A1: The affinity of 9-*cis*RA to CYP26A1 was determined by conducting a Michaelis-Menten kinetic analysis of formation of the primary metabolites. After establishing that product formation was linear with time and protein concentration used, incubations were performed with 11 different concentrations of 9-*cis*RA, between 25 nM and 1 μM. Peak area ratios (primary metabolites quantified as a single peak to internal standard) were plotted against the initial substrate concentrations and the Michaelis-Menten equation was fit to the data using GraphPad Prism (La Jolla, CA). The K_m value was obtained from the fit but the V_{max} was not determined

Downloaded from molpharm.aspetjournals.org at ASPET Journals on April 16, 2024

Molecular Pharmacology Fast Forward. Published on April 26, 2011 as DOI: 10.1124/mol.111.072413
This article has not been copyedited and formatted. The final version may differ from this version.

because the amount of products formed could not be quantified in the absence of reference materials.

Identification of CYP26A1 ligands and calculation of IC_{50} values: Forty-two compounds, as listed in Table 1, were tested as potential inhibitors of CYP26A1. Compounds selected included PPAR and RAR agonists, published RAMBAs, and known P450 inhibitors and probes with wide structural variability, including azole antifungals. Compounds were first tested for inhibition of CYP26A1 mediated 9-*cis*RA hydroxylation at 10 μM concentration. Due to poor ligand solubility, the protease inhibitors were tested at 5 μM. The formation of the primary hydroxylated 9-*cis*RA metabolite eluting at retention time 16.4 min was monitored as a measure of CYP26A1 activity. The percent remaining activity for each inhibitor was calculated by comparing the observed hydroxylation in the test incubations to that measured in controls containing an equal volume of the same solvent as the one in which the inhibitor was dissolved. All incubations were performed in triplicate. To confirm a lack of interference from either the inhibitor or potential metabolites of the inhibitor in the HPLC analysis, the inhibitors were incubated with 5 pmol CYP26A1, 10 pmol reductase, and 1 μM of each ligand for 1 minute in the presence and absence of NADPH and analyzed by HPLC, monitoring wavelengths 360, 280 and 250 nm.

Compounds that showed >10% inhibition of CYP26A1 mediated 9-*cis*RA hydroxylation at 10 μM concentration were also tested at 1 μM to rank the inhibitory effects of the tested ligands and to estimate initial inhibitory potency. IC_{50} values were determined for those compounds that inhibited CYP26A1 activity by more than 50% at 10 μM concentration and showed greater than 10% inhibition at 1 μM concentration. For IC_{50} determination, at least 5 concentrations spanning above and below the predicted IC_{50} were tested and each

Downloaded from molpharm.aspetjournals.org at ASPET Journals on April 16, 2024

Molecular Pharmacology Fast Forward. Published on April 26, 2011 as DOI: 10.1124/mol.111.072413
This article has not been copyedited and formatted. The final version may differ from this version.

concentration was analyzed in duplicate. The IC_{50} values were determined by non-linear regression using GraphPad Prism, according to equation 1:

$$100\% \bullet \frac{v_i}{v} = (\frac{v_i}{v})_{\min} \bullet 100\% + \frac{((v_i/v)_{\max} - (v_i/v)_{\min} \bullet 100\%)}{(1+10^{(I-\log IC_{50})})} \quad (1)$$

in which $100\% \bullet \frac{v_i}{v}$ is the % activity remaining, $(\frac{v_i}{v})_{\max} \bullet 100\%$ is the fitted % maximum activity remaining and $(\frac{v_i}{v})_{\min} \bullet 100\%$ is the % minimum activity remaining. For compounds with IC_{50} values below 100 nM, all fits were corrected for inhibitor depletion and the K_d was determined using the Morrison equation as described in equation 2:

$$[EI] = \frac{[E]+[I]+K_d - \sqrt{([E]+[I]+K_{d)})^2 - 4[E][I]}}{2} \quad (2)$$

in which K_d is the affinity constant of the inhibitor, [I] is the concentration of inhibitor, [E] is the concentration of enzyme, and [EI] is the concentration of the enzyme-inhibitor complex.

Determination of ligand-induced binding spectra and spectral binding constants: To determine whether the identified inhibitors bind within the active site of CYP26A1, ligand induced binding spectra were measured with R115866, R116010 and ketoconazole. For these studies, a 1 mL sample of 0.2 µM CYP26A1 microsomes in 100 mM KPi buffer was split between the sample and reference cuvettes and the binding spectra were measured using an Aminco DW2 Dual Beam spectrophotometer (Olis Instruments, Bogart, GA), scanning from 500 to 375 nm. The inhibitor of interest was added to the sample cuvette until a difference spectrum was observed. An equal volume of solvent was added to the control cuvette. R116010 was tested at 4, 8, 12, 16 and 20 µM and R115866 was tested at 0.2, 0.4, 0.6, 1, 1.2, 1.4, 1.6, 3.6 and 5.2 µM. Ketoconazole was tested at 20,

Downloaded from molpharm.aspetjournals.org at ASPET Journals on April 16, 2024

Molecular Pharmacology Fast Forward. Published on April 26, 2011 as DOI: 10.1124/mol.111.072413
This article has not been copyedited and formatted. The final version may differ from this version.

40, 60, 80, 100 and 120 μM. The absorbance spectra were normalized to 420 or 490 nm for comparison of difference spectra obtained.

Downloaded from molpharm.aspetjournals.org at ASPET Journals on April 16, 2024

Molecular Pharmacology Fast Forward. Published on April 26, 2011 as DOI: 10.1124/mol.111.072413
This article has not been copyedited and formatted. The final version may differ from this version.

Results

Characterization of atRA and 9-cisRA metabolism by CYP26A1: To identify the primary metabolites formed by CYP26A1, *at*RA, *at*RA-d_5, and 9-*cis*RA (Fig 1) were incubated with CYP26A1. Metabolite formation was analyzed by HPLC-UV and detected individual metabolite peaks were collected as HPLC fractions. Molecular ion and MS/MS fragmentation data were collected for each fraction at high mass accuracy (0.3–4 ppm accuracy). Four primary metabolites (peaks 1-4) were formed from *at*RA by CYP26A1 (Fig 2). Three of the atRA metabolites (peaks 1, 3 and 4) had an [M-H] ion of 315.196 *m/z* suggesting that these were hydroxylated metabolites. Two of these metabolites (peaks 1 and 4) lost a deuterium as a result of hydroxylation of *at*RA-d_5 giving a [M-H] ion of 319.221 *m/z.* This suggests that peaks 1 and 4 correspond to hydroxylations at the deuterated carbons, C-4 or C-18. Since the retention time of peak 1 was identical to that of the synthetic 4OH-*at*RA, it was identified as 4OH-*at*RA and peak 4 as 18OH-*at*RA. The third hydroxylation product (peak 3) resulted from a hydroxylation in non-deuterated carbon since in the incubation of *at*RA-d_5 the [M-H] ion was 320.227 *m/z*. The hydroxylation is likely on the β-ionone ring at C-3 or C-16. The synthetic reference material of 3OH-*at*RA eluted at 14.9 minutes (before 4OH-*at*RA at 15.8 min, data not shown), and hence peak 3 could not be 3OH-*at*RA. The dominant MS/MS fragment from peak 3 in *at*RA incubations ([M-H] 315.196 *m/z*) was 241.196 *m/z* in addition to the characteristic loss of CO_2 (loss of 43.989) and H_2O (loss of 18.010) (Fig 2). The 241.196 *m/z* fragment was attributed to the loss of formaldehyde (loss of 30.010) from the 271.206 *m/z* ion instead of ethane which would be a loss of 30.046. The 241.196 *m/z* ion is absent from the 4OH-*at*RA MS/MS spectrum, which is dominated by a loss of CO_2 (loss of 43.989) and loss of H_2O (loss of 18.010) resulting in

Downloaded from molpharm.aspetjournals.org at ASPET Journals on April 16, 2024

Molecular Pharmacology Fast Forward. Published on April 26, 2011 as DOI: 10.1124/mol.111.072413
This article has not been copyedited and formatted. The final version may differ from this version.

fragments at 253.196 *m/z*, 271.206 *m/z* and 297.186 *m/z* (Fig 2). The 241.196 *m/z* fragment is, however, a minor fragment in the MS/MS spectrum of 18OH-*at*RA. In the MS/MS spectrum of peak 3 from *at*RA-d_5 incubation the corresponding fragment is 246.227 retaining all five deuteriums, suggesting a loss of formaldehyde from an undeuterated carbon. The loss of formaldehyde is most likely favored for hydroxylations of a methyl group (C-16 or C-18) in contrast to hydroxylation of the carbons in the β-ionone ring. Based on this data, peak 3 was identified as the 16OH-*at*RA. The fourth metabolite, peak 2 had an [M-H] of 313.180 *m/z* suggesting it is a ketone or an aldehyde. The corresponding metabolite from *at*RA-d_5 had an [M-H] 316.20 m/z suggesting the ketone or aldehyde was at a deuterated position, C-4 or C-18. This metabolite has a similar retention time to synthetic 4oxo-RA, and no loss of formaldehyde was detectable in the MS/MS fragmentation. Loss of formaldehyde would be expected for the 18oxo-RA. Instead, a loss of a CH_3 is detected in the metabolite formed from *at*RA (loss of 15.02 from 269.191 *m/z*) and a loss of CD_3 in the metabolite formed in the incubation with *at*RA-d_5 (loss of 18.042 from 272.209 *m/z*) resulting in the common MS/MS fragment of 254.167 *m/z*. This data suggests that peak 2 is the 4oxo-*at*RA.

All three RA isomers tested, *at*RA, 9-*cis*RA and 13-*cis*RA, were found to be substrates of CYP26A1. No metabolites were observed in the absence of NADPH, absence of protein or absence of substrate. In incubations with 13-*cis*RA, substantial isomerization was observed, preventing characterization of the hydroxylation kinetics of 13-*cis*RA (data not shown). In contrast, 9-*cis*RA underwent minimal isomerization during incubations. A metabolite at the same retention time as 4OH-9*cis*RA reference material was detected (Fig 3A) and minimal secondary metabolism from 9-*cis*RA was observed. Mass spectrometric analysis of the LC fraction of peak at rt 16.5 min showed an [M-H] molecular ion at 315.196 *m/z*, confirming

Downloaded from molpharm.aspetjournals.org at ASPET Journals on April 16, 2024

Molecular Pharmacology Fast Forward. Published on April 26, 2011 as DOI: 10.1124/mol.111.072413
This article has not been copyedited and formatted. The final version may differ from this version.

that this peak is from a hydroxylation product. However, the MS/MS fragmentation data of the metabolite (Fig 3B) showed a significant fragment at 241.196 *m/z,* a fragment that is absent from synthetic 4OH-9*cis*RA (data not shown), but the main fragment in the proposed 16OH-*at*RA. To further characterize this metabolite, LC-MS/MS analysis was employed monitoring two MRM transitions 315>253 *m/z* and 315>241 *m/z* (Fig 3C). This analysis allowed separation of two main metabolites from 9-*cis*RA. The first one was mainly detected at the 315>253 channel and had an identical MS/MS fragmentation pattern of the 315 *m/z* as synthetic 4OH-9*cis*RA (Fig3C). The second metabolite was detected mainly on the 315>241 channel and had a fragmentation pattern similar to the tentatively identified 16OH-*at*RA (Fig 3C). Based on this data it was concluded that at least two hydroxylation products are formed from 9-*cis*RA by CYP26A1 and the high resolution MS/MS spectrum is a combination of two coeluting metabolites. The overall fragmentation pattern for the hydroxylated metabolites is shown in Fig 3D.

Identification of CYP26A1 inhibitors and determination of IC_{50} values: The apparent K_m for 9-*cis*RA metabolism by CYP26A1 was determined to establish appropriate substrate concentration for the inhibition assay (Fig 3E). The K_m for the formation of the hydroxylated metabolites (quantified by UV as a single peak) of 9-*cis*RA was 134 ± 30 nM. Based on this experimentally determined K_m, further incubations to identify and characterize potential inhibitors were performed at 100 nM 9-*cis*RA.

Forty-two compounds were screened for CYP26A1 inhibition (Table 1). Twenty-one of these compounds resulted in >10% inhibition of 9-*cis*RA hydroxylation at 10 μM concentration (Fig 4A and B). Eleven of these 21 compounds also inhibited CYP26A1 by

Downloaded from molpharm.aspetjournals.org at ASPET Journals on April 16, 2024

Molecular Pharmacology Fast Forward. Published on April 26, 2011 as DOI: 10.1124/mol.111.072413
This article has not been copyedited and formatted. The final version may differ from this version.

>10% at 1 μM (Fig 4C and D). IC_{50} values (Table 2) were determined for all compounds that had >20% inhibition at 1 μM and for CS5, pioglitazone and rosiglitazone.

The two compounds that were designed as inhibitors of *at*RA metabolism, R116010 and R115866 (Fig 5) were the most potent inhibitors of CYP26A1 with low nanomolar K_d values (Table 2 and Fig 5). The IC_{50} value of ketoconazole (IC_{50} = 0.5 μM) was about 100-fold higher, and the IC_{50} of liarozole (IC_{50} = 2.1 μM) about 500-fold higher than those of R115866 and R116010 (Table 2 and Fig 5). The IC_{50} values of other azoles (fluconazole, itraconazole and voriconazole) appeared to be >10 μM, based on the <50% inhibition at 10 μM concentration. The two inhibitors of RA metabolism lacking triazole or imidazole groups, CS5 and CS6 (Fig 6), were less potent inhibitors of CYP26A1 than R115866, R116010 and ketoconazole but CS5 had a similar IC_{50} as liarozole.

Some of the tested RAR agonists also bound to CYP26A1 and inhibited the hydroxylation of 9-*cis*RA, but large differences in the binding affinity of the RAR agonists were observed. Of the RAR agonists tested, the most potent inhibitor was CD1530 (IC_{50} = 0.5 μM), an RARγ selective agonist (Table 2 and Fig 6), which was equipotent with ketoconazole. TTNPB, a pan-RAR agonist, had a 10-fold higher IC_{50} (3.7 μM) as a CYP26A1 inhibitor than CD1530, and the RARβ selective agonist AC55649 did not inhibit CYP26A1 even at 10 μM concentration. AM580, an RARα specific agonist, inhibited CYP26A1 by 58% at 10 μM concentration but not at all at 1 μM. The two PPARγ agonists rosiglitazone and pioglitazone and the PPARβ/δ selective agonist L-165,041 inhibited CYP26A1 with approximately equal potency, with IC_{50} values between 1.7 and 8.6 μM (Fig 6). However, the PPARγ selective irreversible antagonist GW9662 did not have appreciable effects on CYP26A1 activity at 10 μM, despite the shared PPAR binding affinity.

Downloaded from molpharm.aspetjournals.org at ASPET Journals on April 16, 2024

Molecular Pharmacology Fast Forward. Published on April 26, 2011 as DOI: 10.1124/mol.111.072413
This article has not been copyedited and formatted. The final version may differ from this version.

Determination of ligand-induced binding spectra: To determine if the identified azole inhibitors bind within the CYP26A1 active site and whether a triazole or imidazole nitrogen coordinates to the heme iron, ligand-induced binding spectra were obtained using CYP26A1 insect cell microsomes (Fig 7). R115866, R116010, and ketoconazole binding resulted in a type II binding spectra characterized by a high to low spin shift of the heme iron. Interestingly, the minima and maxima of these spectra were shifted towards longer wavelengths when compared to classic type II spectra. The observed minima were between 400 and 415 nm, and the maxima were between 425 and 440 nm, and they increased with increasing concentrations.

Downloaded from molpharm.aspetjournals.org at ASPET Journals on April 16, 2024

Molecular Pharmacology Fast Forward. Published on April 26, 2011 as DOI: 10.1124/mol.111.072413
This article has not been copyedited and formatted. The final version may differ from this version.

Discussion

CYP26A1 is one of the main enzymes responsible for *at*RA hydroxylation but the metabolites generated from *at*RA by CYP26A1 have been only partially identified (Chithalen et al., 2002; Lutz et al., 2009; White et al., 1997). This study showed that 4OH-*at*RA and 18OH-*at*RA as well as 4oxo-*at*RA are formed by CYP26A1. This is in agreement with previous data obtained from cell culture systems (Chithalen et al., 2002). However, in contrast to previously proposed formation of 3OH-*at*RA, our data show that 3OH-*at*RA is not a metabolite formed by CYP26A1, but instead that 16OH-*at*RA is the most likely third hydroxylation product. 16OH-*at*RA has been reported as the main *at*RA hydroxylation product formed by CYP120A1, the cyanobacterial *at*RA hydroxylase homologous to CYP26A1 (Alder et al., 2009). 16OH-*at*RA has also shown as a metabolite of *at*RA in *at*RA induced T47D cells and its formation was inhibited by R116010 (van Heusden et al., 2002). The oxidation of C16 likely results from rotation of the bond connecting the β-ionone ring to the linear isoprenoid side chain placing the C16 near the heme similar to C4. This orientation is shown in the crystal structure of CYP120A1 in which C16 is at 4.4Å from the heme (Kühnel et al., 2008). In a previous study, 4oxo-*at*RA was not detected as a metabolite in incubations of 4OH-*at*RA and CYP26A1 (Lutz et al., 2009). Hence it is surprising that 4oxo-*at*RA was detected in the current study. Further studies of the sequential dissociative and nondissociative metabolism of *at*RA by CYP26A1 are needed to explain this discrepancy.

In addition to *at*RA, 9-*cis*RA was a substrate of CYP26A1, which is in contrast to the lack of hydroxylation of 9-*cis*RA in transfected HCT 116-hCYP26 cells (Sonneveld et al., 1998). 9-*cis*RA is a substrate of CYP26C1 (Taimi et al., 2004) with the 4OH-9*cis*RA identified as

Downloaded from molpharm.aspetjournals.org at ASPET Journals on April 16, 2024

Molecular Pharmacology Fast Forward. Published on April 26, 2011 as DOI: 10.1124/mol.111.072413
This article has not been copyedited and formatted. The final version may differ from this version.

the main metabolite. The metabolism of 9-*cis*RA by CYP26A1 also resulted in formation of 4OH-9*cis*RA, but the high-resolution MS/MS data as well as the LC-MS/MS data show that a second hydroxylation product, most likely 16OH-9*cis*RA, is formed. Interestingly, despite the high affinity of 9-*cis*RA and *at*RA to CYP26A1 and the ligand selectivity of CYP26A1, multiple hydroxylation products are observed from both 9-*cis*RA and *at*RA suggesting that both substrates have multiple binding orientations in the CYP26A1 active site. Despite the formation of two metabolites from 9-*cis*RA, 9-*cis*RA hydroxylation is a better probe for testing CYP26A1 inhibition than *at*RA metabolism. The key advantages of using 9-*cis*RA instead of *at*RA for measuring inhibition of CYP26A1 are the lower binding affinity of 9-*cis*RA to CYP26A1, and lack of substantial sequential metabolism and product depletion.

Using 9-*cis*RA hydroxylation as a probe, twenty-one potential inhibitors of CYP26A1 were identified from a wide variety of compounds. With the exception of ketoconazole, the compounds selected from classic P450 substrates and inhibitors either did not inhibit CYP26A1 or inhibited it weakly, demonstrating that CYP26A1 has high ligand selectivity. Also with the exception of ketoconazole, the compounds with high affinity (<1 μM IC_{50}) for CYP26A1 were designed either as inhibitors of RA metabolism or as RAR agonists using *at*RA as the lead structure.

Overall, the RAR agonists had lower affinity for CYP26A1 than for RAR isoforms. An exception was CD1530, which had a similar binding affinity towards CYP26A1 as reported for RARγ (Thacher et al., 2000), and higher affinity for CYP26A1 than for RARα and RARβ isoforms. In cell systems, CD1530 is expected to inhibit CYP26A1 at similar concentrations as those required for RARγ activation. TTNPB and AM580 had lower binding affinities toward CYP26A1 than reported for RAR isoforms (Thacher et al., 2000), but it is possible

Downloaded from molpharm.aspetjournals.org at ASPET Journals on April 16, 2024

Molecular Pharmacology Fast Forward. Published on April 26, 2011 as DOI: 10.1124/mol.111.072413
This article has not been copyedited and formatted. The final version may differ from this version.

that when used in cell systems these compounds also inhibit CYP26A1. This is an important finding as CYP26A1 inhibition leading to increased concentrations of *at*RA in cells simultaneously with RAR activation, could confound results in RAR activation assays and mask the mechanism of cellular effects.

Our findings confirm previous studies showing that R115866 and R116010 inhibit *at*RA metabolism with high affinity. R115866 had an IC_{50} of 4nM and 5nM when tested in yeast and MCF-7 cells expressing CYP26A1, respectively (Stoppie et al., 2000), and R116010 had an IC_{50} of 8.7nM in human T47D breast cancer cells induced with *at*RA (Van Heusden et al., 2002). The inhibitory potency of ketoconazole towards CYP26A1 in this study was much higher (IC_{50} = 0.5µM) than previously observed (IC_{50}-values 18 and 12µM in rat liver microsomes and MCF-7 cells, respectively). The inhibitory potency of CS5 was in good agreement with previous studies. The IC_{50}-value for CS5 was >20µM when tested in rat liver microsomes and 7µM when tested in *at*RA induced MCF-7 cells (Yee et al., 2005). In MCF-7 cells and rat liver microsomes, CS6 was a more potent inhibitor than CS5 (IC_{50} 0.4 and 5µM in rat liver microsomes and MCF-7 cells, respectively) and was suggested to have more broad inhibition potential than CS5 (Yee et al., 2005). In our study, CS6 inhibited CYP26A1 activity <20% when tested at 10µM in comparison to 50% inhibition by CS5. A possible explanation for these discrepancies is the contribution of other enzymes to atRA metabolism in rat liver microsomes and/or MCF-7 cells or differences in nonspecific binding of the inhibitors in different systems. The differences in inhibitory potencies between the systems highlight the need of determining initial inhibition constants using a single enzyme system. This is especially important when reliable selective probe substrates are not available for the specific CYP isoform. Because *at*RA is metabolized by multiple CYP

Downloaded from molpharm.aspetjournals.org at ASPET Journals on April 16, 2024

Molecular Pharmacology Fast Forward. Published on April 26, 2011 as DOI: 10.1124/mol.111.072413
This article has not been copyedited and formatted. The final version may differ from this version.

enzymes (Thatcher et al., 2010), the contribution of each isoform is expected to vary between different tissues and cell types. At present, the predominant CYP26 isoform expressed in MCF-7 cells and the selectivity of the inhibitors for different CYP26 isoforms are unknown.

The result that ketoconazole is 4-fold more potent CYP26A1 inhibitor than liarozole is in contrast with what was expected from *in vivo* findings (Van Wauwe et al., 1990). In rats, when administered at similar doses, liarozole caused an approximately 3-fold increase in *at*RA AUC whereas ketoconazole only increased *at*RA concentrations 1.5-fold (Van Wauwe et al., 1990). This discrepancy is most likely due to different circulating free concentrations of ketoconazole and liarozole resulting from different plasma protein binding, clearance and volume of distribution. In agreement with our data, both liarozole and ketoconazole have been shown to inhibit *at*RA metabolism *in vitro* in hamster or rat liver microsomes (Van Wauwe et al., 1992; Van Wauwe et al., 1988). Also, no potent CYP26A1 inhibition was observed by itraconazole in this study, similar to the data that itraconazole did not inhibit *at*RA metabolism *in vivo* in rats (Van Wauwe et al., 1990).

The finding that ketoconazole is a potent inhibitor of CYP26A1 is consistent with clinical findings that *at*RA dose needs to be decreased when *at*RA is co-administered with ketoconazole or fluconazole. When ketoconazole was administered on day 28 of *at*RA therapy, a 72% increase in plasma AUC of *at*RA was observed (Rigas et al., 1993), suggesting a <50% decrease in the clearance of *at*RA. The finding that fluconazole (C_{max} 43.6μM (Debruyne and Ryckelynck, 1993)) is a weak CYP26A1 inhibitor (IC_{50}>10μM) does not explain the 2–4 fold increase in *at*RA AUC (Schwartz et al., 1995) or a need to decrease *at*RA dose by 70% (Vanier et al., 2003) after fluconazole administration. This suggests that

Downloaded from molpharm.aspetjournals.org at ASPET Journals on April 16, 2024

Molecular Pharmacology Fast Forward. Published on April 26, 2011 as DOI: 10.1124/mol.111.072413
This article has not been copyedited and formatted. The final version may differ from this version.

CYP26A1 is not the only enzyme clearing *at*RA in humans. It is possible that fluconazole causes the interaction by inhibiting other CYP26 isoforms or CYP2C and CYP3A enzymes.

It is surprising that the PPARγ and PPARβ/δ agonists pioglitazone, rosiglitazone and L165,041 inhibited CYP26A1 with similar potency as liarozole. In previous studies pioglitazone and rosiglitazone were found to induce CYP26B1 mRNA in HepG2 cells (Tay et al., 2010) but they have not previously been shown to affect *at*RA metabolism. Since pioglitazone and rosiglitazone plasma concentrations reach low μM (C_{max}) values after clinical administration, it is possible that these drugs cause weak-to-moderate inhibition of *at*RA metabolism *in vivo*. This is of interest since pioglitazone and rosiglitazone are used for treatment of diabetes and 9-*cis*RA was recently shown to play a role in regulation of blood glucose (Kane et al., 2010). It is possible that inhibition of 9-*cis*RA metabolism in the pancreas also plays a role in pioglitazone's and rosiglitazone's activity.

In conclusion, this study shows that CYP26A1 has high ligand selectivity, but can be inhibited by retinoids and other structurally related drugs. This study also shows that 9-*cis*RA and 13-*cis*RA are substrates for CYP26A1 suggesting that CYP26A1 has a role in inactivating bioactive retinoids. This finding may be important in further understanding of retinoid biochemistry. Future studies screening a larger panel of retinoids and RAR agonists are needed to determine the extent of ligand overlap between RAR isoforms and CYP26 enzymes. Based on the presented data, RAR, PPAR and CYP26A1 have considerable ligand overlap, suggesting that inhibition of CYP26A1, leading to increased *at*RA concentrations, could contribute to the biological activity of RAR and PPAR agonists.

Downloaded from molpharm.aspetjournals.org at ASPET Journals on April 16, 2024

Molecular Pharmacology Fast Forward. Published on April 26, 2011 as DOI: 10.1124/mol.111.072413
This article has not been copyedited and formatted. The final version may differ from this version.

Acknowledgements

The authors wish to thank Ms. Jessica Tay, Dr. Vaishali Dixit and Dr. Alex Zelter for their assistance in CYP26 expression and in conducting preliminary experiments of CYP26A1 inhibition and metabolism and Dr Justin D Lutz for his assistance in the LC-MS/MS experiments. The authors also wish to thank Dr. William Atkins and Rob Foti for their assistance in the selection of broad range substrates to screen as potential inhibitors of CYP26.

Downloaded from molpharm.aspetjournals.org at ASPET Journals on April 16, 2024

Molecular Pharmacology Fast Forward. Published on April 26, 2011 as DOI: 10.1124/mol.111.072413
This article has not been copyedited and formatted. The final version may differ from this version.

Authorship Contributions

Participated in research design: Thatcher, Nelson, Isoherranen

Conducted experiments: Thatcher, Buttrick, Shaffer, Isoherranen

Contributed new reagents or analytic tools: Shimshoni, Goodlett

Performed data analysis: Thatcher, Buttrick, Shaffer, Goodlett, Nelson, Isoherranen

Wrote or contributed to the writing of the manuscript: Thatcher, Shaffer, Nelson, Isoherranen

Downloaded from molpharm.aspetjournals.org at ASPET Journals on April 16, 2024

Molecular Pharmacology Fast Forward. Published on April 26, 2011 as DOI: 10.1124/mol.111.072413
This article has not been copyedited and formatted. The final version may differ from this version.

References

Alder, A., Bigler, P., Werck-Reichhart, D., Al-Babili, S. (2009). In vitro characterization of Synechocystis CYP120A1 revealed the first nonanimal retinoic acid hydroxylase FEBS J 276, 5416-5431.

Altucci, L., Leibowitz, M. D., Ogilvie, K. M., de Lera, A. R., and Gronemeyer, H. (2007). RAR and RXR modulation in cancer and metabolic disease. Nat Rev Drug Discov *6*, 793-810.

Barua, R. K., and Barua, A. B. (1964). Vitamin A acid from retinene. The Biochemical journal *92*, 21C-22C.

Blomhoff, R., and Blomhoff, H. K. (2006). Overview of retinoid metabolism and function. J Neurobiol *66*, 606-630.

Chithalen, J. V., Luu, L., Petkovich, M., and Jones, G. (2002). HPLC-MS/MS analysis of the products generated from all-trans-retinoic acid using recombinant human CYP26A. J Lipid Res *43*, 1133-1142.

Debruyne, D., and Ryckelynck, J. P. (1993). Clinical pharmacokinetics of fluconazole. Clin Pharmacokinet *24*, 10-27.

Duester, G. (2008). Retinoic acid synthesis and signaling during early organogenesis. Cell *134*, 921-931.

Garattini, E., Gianni, M., and Terao, M. (2007). Retinoids as differentiating agents in oncology: a network of interactions with intracellular pathways as the basis for rational therapeutic combinations. Curr Pharm Des *13*, 1375-1400.

Gomaa, M. S., Yee, S. W., Milbourne, C. E., Barbera, M. C., Simons, C., and Brancale, A. (2006). Homology model of human retinoic acid metabolising enzyme

Downloaded from molpharm.aspetjournals.org at ASPET Journals on April 16, 2024

Molecular Pharmacology Fast Forward. Published on April 26, 2011 as DOI: 10.1124/mol.111.072413
This article has not been copyedited and formatted. The final version may differ from this version.

cytochrome P450 26A1 (CYP26A1): active site architecture and ligand binding. Journal of enzyme inhibition and medicinal chemistry *21*, 361-369.

Jacobs, S., Lie, D. C., DeCicco, K. L., Shi, Y., DeLuca, L. M., Gage, F. H., and Evans, R. M. (2006). Retinoic acid is required early during adult neurogenesis in the dentate gyrus. Proc Natl Acad Sci U S A *103*, 3902-3907.

Kane, M. A., Folias, A. E., Pingitore, A., Perri, M., Obrochta, K. M., Krois, C. R., Cione, E., Ryu, J. Y., and Napoli, J. L. (2010). Identification of 9-cis-retinoic acid as a pancreas-specific autacoid that attenuates glucose-stimulated insulin secretion. Proc Natl Acad Sci U S A *107*, 21884-21889.

Kane, M. A., Folias, A. E., Wang, C., and Napoli, J. L. (2008). Quantitative profiling of endogenous retinoic acid in vivo and in vitro by tandem mass spectrometry. Anal Chem *80*, 1702-1708.

Karlsson M., Strid. A., Sirsjo A., Eriksson L. A. (2008). Homology Models and Molecular Modeling of Human Retinoic Acid Metabolizing Enzymes Cytochrome P450 26A1 (CYP26A1) and P450 26B1 (CYP26B1). J Chem Theory Comput *4*, 1021–1027.

Kühnel, K., Ke, N., Cryle, M. J., Sligar, S. G., Schuler, M. A., Schlichting, I. (2008). Crystal structures of substrate-free and retinoic acid-bound cyanobacterial cytochrome P450 CYP120A1 Biochemistry 47,6552-6559.

Lutz, J. D., Dixit, V., Yeung, C. K., Dickmann, L. J., Zelter, A., Thatcher, J. E., Nelson, W. L., and Isoherranen, N. (2009). Expression and functional characterization of cytochrome P450 26A1, a retinoic acid hydroxylase. Biochem Pharmacol *77*, 258-268.

Muindi, J., Frankel, S. R., Miller, W. H., Jr., Jakubowski, A., Scheinberg, D. A., Young, C. W., Dmitrovsky, E., and Warrell, R. P., Jr. (1992). Continuous treatment with all-

Downloaded from molpharm.aspetjournals.org at ASPET Journals on April 16, 2024

Molecular Pharmacology Fast Forward. Published on April 26, 2011 as DOI: 10.1124/mol.111.072413
This article has not been copyedited and formatted. The final version may differ from this version.

trans retinoic acid causes a progressive reduction in plasma drug concentrations: implications for relapse and retinoid "resistance" in patients with acute promyelocytic leukemia. Blood *79*, 299-303.

Mulvihill, M. J., Kan, J. L., Beck, P., Bittner, M., Cesario, C., Cooke, A., Keane, D. M., Nigro, A. I., Nillson, C., Smith, V., *et al.* (2005). Potent and selective [2-imidazol-1-yl-2-(6-alkoxy-naphthalen-2-yl)-1-methyl-ethyl]-dimethyl-ami nes as retinoic acid metabolic blocking agents (RAMBAs). Bioorg Med Chem Lett *15*, 1669-1673.

Njar, V. C., Gediya, L., Purushottamachar, P., Chopra, P., Vasaitis, T. S., Khandelwal, A., Mehta, J., Huynh, C., Belosay, A., and Patel, J. (2006). Retinoic acid metabolism blocking agents (RAMBAs) for treatment of cancer and dermatological diseases. Bioorg Med Chem *14*, 4323-4340.

Patel, J. B., Huynh, C. K., Handratta, V. D., Gediya, L. K., Brodie, A. M., Goloubeva, O. G., Clement, O. O., Nanne, I. P., Soprano, D. R., and Njar, V. C. (2004). Novel retinoic acid metabolism blocking agents endowed with multiple biological activities are efficient growth inhibitors of human breast and prostate cancer cells in vitro and a human breast tumor xenograft in nude mice. J Med Chem *47*, 6716-6729.

Petkovich, M., Brand, N. J., Krust, A., and Chambon, P. (1987). A human retinoic acid receptor which belongs to the family of nuclear receptors. Nature *330*, 444-450.

Ren, J. H., Xiong, X. Q., Sha, Y., Yan, M. C., Lin, B., Wang, J., Jing, Y. K., Zhao, D. M., and Cheng, M. S. (2008). Structure prediction and R115866 binding study of human CYP26A1: homology modelling, fold recognition, molecular docking and MD simulations. Molecular Simulation *34*, 337-346.

Downloaded from molpharm.aspetjournals.org at ASPET Journals on April 16, 2024

Molecular Pharmacology Fast Forward. Published on April 26, 2011 as DOI: 10.1124/mol.111.072413
This article has not been copyedited and formatted. The final version may differ from this version.

Rigas, J. R., Francis, P. A., Muindi, J. R., Kris, M. G., Huselton, C., DeGrazia, F., Orazem, J. P., Young, C. W., and Warrell, R. P., Jr. (1993). Constitutive variability in the pharmacokinetics of the natural retinoid, all-trans-retinoic acid, and its modulation by ketoconazole. J Natl Cancer Inst *85*, 1921-1926.

Schwartz, E. L., Hallam, S., Gallagher, R. E., and Wiernik, P. H. (1995). Inhibition of all-trans-retinoic acid metabolism by fluconazole in vitro and in patients with acute promyelocytic leukemia. Biochem Pharmacol *50*, 923-928.

Sonneveld, E., van den Brink, C. E., van der Leede, B. M., Schulkes, R. K., Petkovich, M., van der Burg, B., and van der Saag, P. T. (1998). Human retinoic acid (RA) 4-hydroxylase (CYP26) is highly specific for all-trans-RA and can be induced through RA receptors in human breast and colon carcinoma cells. Cell Growth Differ *9*, 629-637.

Stoppie, P., Borgers, M., Borghgraef, P., Dillen, L., Goossens, J., Sanz, G., Szel, H., Van Hove, C., Van Nyen, G., Nobels, G., *et al.* (2000). R115866 inhibits all-trans-retinoic acid metabolism and exerts retinoidal effects in rodents. J Pharmacol Exp Ther *293*, 304-312.

Taimi, M., Helvig, C., Wisniewski, J., Ramshaw, H., White, J., Amad, M., Korczak, B., and Petkovich, M. (2004). A novel human cytochrome P450, CYP26C1, involved in metabolism of 9-cis and all-trans isomers of retinoic acid. J Biol Chem *279*, 77-85.

Tang, X. H., and Gudas, L. J. (2011). Retinoids, retinoic acid receptors, and cancer. Annu Rev Pathol *6*, 345-364.

Tay, S., Dickmann, L., Dixit, V., and Isoherranen, N. (2010). A comparison of the roles of peroxisome proliferator-activated receptor and retinoic acid receptor on CYP26 regulation. Mol Pharmacol *77*, 218-227.

Downloaded from molpharm.aspetjournals.org at ASPET Journals on April 16, 2024

Molecular Pharmacology Fast Forward. Published on April 26, 2011 as DOI: 10.1124/mol.111.072413
This article has not been copyedited and formatted. The final version may differ from this version.

Thacher, S. M., Vasudevan, J., and Chandraratna, R. A. (2000). Therapeutic applications for ligands of retinoid receptors. Curr Pharm Des *6*, 25-58.

Thatcher, J. E., Zelter, A., and Isoherranen, N. (2010). The relative importance of CYP26A1 in hepatic clearance of all-trans retinoic acid. Biochemical pharmacology *80*, 903-912.

van der Leede, B. M., van den Brink, C. E., Pijnappel, W. W., Sonneveld, E., van der Saag, P. T., and van der Burg, B. (1997). Autoinduction of retinoic acid metabolism to polar derivatives with decreased biological activity in retinoic acid-sensitive, but not in retinoic acid-resistant human breast cancer cells. J Biol Chem *272*, 17921-17928.

Van Heusden, J., Van Ginckel, R., Bruwiere, H., Moelans, P., Janssen, B., Floren, W., van der Leede, B. J., van Dun, J., Sanz, G., Venet, M., *et al.* (2002). Inhibition of all-TRANS-retinoic acid metabolism by R116010 induces antitumour activity. Br J Cancer *86*, 605-611.

Van Wauwe, J., Van Nyen, G., Coene, M. C., Stoppie, P., Cools, W., Goossens, J., Borghgraef, P., and Janssen, P. A. (1992). Liarozole, an inhibitor of retinoic acid metabolism, exerts retinoid-mimetic effects in vivo. J Pharmacol Exp Ther *261*, 773-779.

Van Wauwe, J. P., Coene, M. C., Goossens, J., Cools, W., and Monbaliu, J. (1990). Effects of cytochrome P-450 inhibitors on the in vivo metabolism of all-trans-retinoic acid in rats. J Pharmacol Exp Ther *252*, 365-369.

Van Wauwe, J. P., Coene, M. C., Goossens, J., Van Nijen, G., Cools, W., and Lauwers, W. (1988). Ketoconazole inhibits the in vitro and in vivo metabolism of all-trans-retinoic acid. J Pharmacol Exp Ther *245*, 718-722.

Downloaded from molpharm.aspetjournals.org at ASPET Journals on April 16, 2024

Molecular Pharmacology Fast Forward. Published on April 26, 2011 as DOI: 10.1124/mol.111.072413
This article has not been copyedited and formatted. The final version may differ from this version.

Vanier, K. L., Mattiussi, A. J., and Johnston, D. L. (2003). Interaction of all-trans-retinoic acid with fluconazole in acute promyelocytic leukemia. J Pediatr Hematol Oncol *25*, 403-404.

White, J. A., Beckett-Jones, B., Guo, Y. D., Dilworth, F. J., Bonasoro, J., Jones, G., and Petkovich, M. (1997). cDNA cloning of human retinoic acid-metabolizing enzyme (hP450RAI) identifies a novel family of cytochromes P450. J Biol Chem *272*, 18538-18541.

White, J. A., Guo, Y. D., Baetz, K., Beckett-Jones, B., Bonasoro, J., Hsu, K. E., Dilworth, F. J., Jones, G., and Petkovich, M. (1996). Identification of the retinoic acid-inducible all-trans-retinoic acid 4-hydroxylase. J Biol Chem *271*, 29922-29927.

Wouters, W., van Dun, J., Dillen, A., Coene, M. C., Cools, W., and De Coster, R. (1992). Effects of liarozole, a new antitumoral compound, on retinoic acid-induced inhibition of cell growth and on retinoic acid metabolism in MCF-7 human breast cancer cells. Cancer Res *52*, 2841-2846.

Yee, S. W., Jarno, L., Gomaa, M. S., Elford, C., Ooi, L. L., Coogan, M. P., McClelland, R., Nicholson, R. I., Evans, B. A., Brancale, A., and Simons, C. (2005). Novel tetralone-derived retinoic acid metabolism blocking agents: synthesis and in vitro evaluation with liver microsomal and MCF-7 CYP26A1 cell assays. J Med Chem *48*, 7123-7131.

Downloaded from molpharm.aspetjournals.org at ASPET Journals on April 16, 2024

Molecular Pharmacology Fast Forward. Published on April 26, 2011 as DOI: 10.1124/mol.111.072413
This article has not been copyedited and formatted. The final version may differ from this version.

Footnotes

This work was supported by National Institute of General Medical Sciences Grants [T32 GM007750], [R01 GM081569] and [R01 GM081569-S1].

Reprint requests: Nina Isoherranen, Department of Pharmaceutics, Box 357610, University of Washington, Seattle, WA 98195. E-mail: ni2@u.washington.edu

Downloaded from molpharm.aspetjournals.org at ASPET Journals on April 16, 2024

Molecular Pharmacology Fast Forward. Published on April 26, 2011 as DOI: 10.1124/mol.111.072413
This article has not been copyedited and formatted. The final version may differ from this version.

Legends for Figures:

Fig 1. Chemical structures of RA isomers, *at*RA-d_5, and detected or proposed *at*RA metabolites.

Fig 2. Characterization of metabolites of *at*RA formed by CYP26A1. HPLC-UV chromatograms of the metabolites formed after incubating *at*RA (top panel) or *at*RA-d_5(bottom panel) at 100 μM concentration with 100 pmol CYP26A1 for 1 hour. The peaks labeled as 1, 2, 3 and 4 were collected as HPLC fractions and analyzed by high-resolution mass spectrometry as described in materials and methods. The MS/MS spectra of the four fractions are shown with the [M-H] ion *m/z* listed as an inset to the spectrum. The four metabolites were identified as peak 1, 4OH-*at*RA; peak 2 4oxo-*at*RA; peak 3 16OH-*at*RA and peak 4, 18OH-*at*RA.

Fig 3. Characterization of 9-*cis*RA as a substrate of CYP26A1. An HPLC chromatogram of the metabolites formed from 9-*cis*RA (100 μM) with 100 pmol CYP26A1 (A). The peak at 16.5 min depicted in panel A was collected for MS/MS analysis. Panel B shows the high resolution MS/MS spectrum of [M-H] 315 *m/z* of this peak. Panel C shows a further characterization of the 9-*cis*RA metabolites detected by LC-MS/MS as described in materials and methods. The black trace shows the MRM chromatogram of m/z transition 315>253 and the red trace shows the m/z transition 315>241. Retention times are not comparable between panels A and C due to different HPLC separation condition used. The insets show the MS/MS spectra acquired from m/z 315 for the two overlapping peaks demonstrating the presence of two different metabolites. The proposed fragmentation pathway of the hydroxylated 9-*cis*RA metabolites is shown in panel D. Panel E shows the determination of the Michaelis-Menten constant (K_m) for 9-*cis*RA hydroxylation by CYP26A1 using 5 pmol CYP26A1, 10 pmol reductase, and 9-*cis*RA concentrations 25 nM – 1 μM. Incubation times were 1 minute. The K_m was determined to be 134 nM.

Fig 4. Percent inhibition of CYP26A1 mediated 9-*cis*RA hydroxylation by identified ligands. The inhibition of CYP26A1 by a diverse selection of compounds (A and C) and select retinoids, RAMBAs and RAR agonists (B and D). The top panels (A and B) show the inhibition at 10 μM inhibitor concentration and the bottom panels show inhibition at 1 μM inhibitor concentration (C and D) with 9-*cis*RA (100 nM) as substrate.

Fig 5. Determination of IC_{50} values for azole inhibitors of CYP26A1, and the relevant structures. IC_{50} values were calculated by incubating 5 pmol CYP26A1, 10 pmol reductase, 100 nM 9-*cis*RA and at least 5 concentrations of inhibitor. The % activity remaining or concentration of the enzyme inhibitor complex was calculated and plotted against inhibitor concentration. The Morrison equation (Equation 2) was fit to the R115866 and R116010 data. Equation 1 was fitted to the liarozole and ketoconazole data.

Fig 6. Determination of IC_{50} values for PPAR and RAR ligands and CS5 towards CYP26A1 mediated 9-*cis*RA oxidation. The structures of the inhibitors are shown as inserts. IC_{50} values were calculated by incubating 5 pmol CYP26A1, 10 pmol reductase, 100 nM 9-*cis*RA and at least 5 concentrations of inhibitor. The % activity remaining was calculated and plotted against inhibitor concentration and Equation 1 was fitted to the data.

Downloaded from molpharm.aspetjournals.org at ASPET Journals on April 16, 2024

Molecular Pharmacology Fast Forward. Published on April 26, 2011 as DOI: 10.1124/mol.111.072413
This article has not been copyedited and formatted. The final version may differ from this version.

Fig 7. Ligand induced difference spectra for ketoconazole, R116010, and R115866 binding to CYP26A1. All spectra were recorded as described in Materials and Methods.

Downloaded from molpharm.aspetjournals.org at ASPET Journals on April 16, 2024

Molecular Pharmacology Fast Forward. Published on April 26, 2011 as DOI: 10.1124/mol.111.072413
This article has not been copyedited and formatted. The final version may differ from this version.

Tables:

Table 1. Summary of compounds screened as potential inhibitors of CYP26A1. Compounds were assigned as "positive" if they inhibited CYP26A1 more than 10% when tested at 10 μM.

Screen positive	Screen negative
R115866	AC 55649
R116010	nelfinavir
liarozole	quinidine
ketoconazole	lopinavir
fluconazole	simvastatin
itraconazole	diltiazem
voriconazole	methoxypsoralen
terfenadine	darunavir
danazol	erythromycin
tamoxifen	verapamil
pimozide	propranolol
tipranavir	atazanavir
CS6	omeprazole
CS5	indinavir
CD 1530	saquinavir
TTNPB	ranolazine
L-165,041	paclitaxel
rosiglitazone	cyclosporine
pioglitazone	quinapril
AM 580	amprenavir
GW 9662	ritonavir

Downloaded from molpharm.aspetjournals.org at ASPET Journals on April 16, 2024

Molecular Pharmacology Fast Forward. Published on April 26, 2011 as DOI: 10.1124/mol.111.072413
This article has not been copyedited and formatted. The final version may differ from this version.

Table 2. IC_{50} values for inhibitors of CYP26A1. IC_{50} values were obtained from the fits of the data shown in Figures 5 and 6.

Compound	IC_{50} or K_d, in µM (SE)
R116010	0.0043 (0.0007)
R115866	0.0051 (0.0008)
CD 1530	0.53 (1.9)
ketoconazole	0.55 (1.3)
L-165,041	1.7 (1.6)
liarozole	2.1 (1.1)
CS5	2.6 (1.3)[a]
TTNPB	3.7 (1.6)
rosiglitazone	4.2 (1.3)
pioglitazone	8.6 (1.2)

[a]The IC_{50} value is determined as 50% inhibition of the maximum 71% inhibition observed.

Downloaded from molpharm.aspetjournals.org at ASPET Journals on April 16, 2024

Figure 1

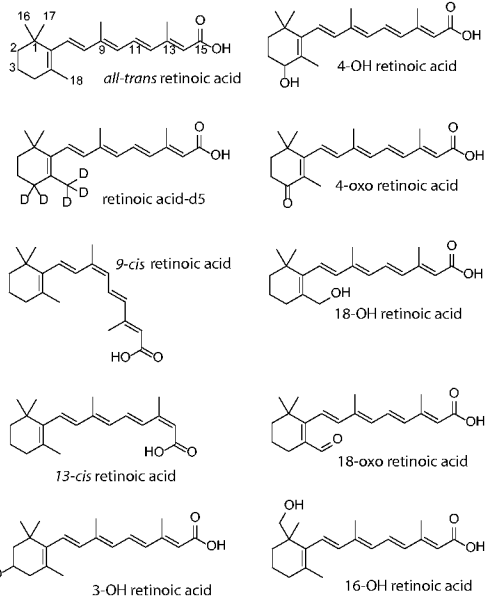
16
17
2
1
3
9
11
13
15
OH
18
all-trans retinoic acid
4-OH retinoic acid
OH
D
D
D
D
D
retinoic acid-d5
4-oxo retinoic acid
9-cis retinoic acid
HO
18-OH retinoic acid
13-cis retinoic acid
18-oxo retinoic acid
3-OH retinoic acid
16-OH retinoic acid

Figure 2

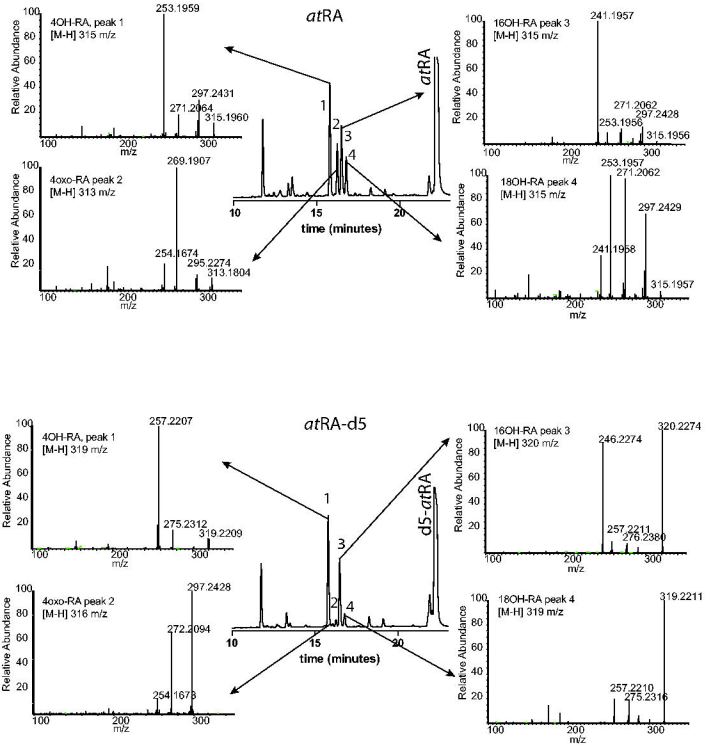
atRA
4OH-RA, peak 1
[M-H] 315 m/z
253.1959
297.2431
271.2064
315.1960
4oxo-RA peak 2
[M-H] 313 m/z
269.1907
254.1674
295.2274
313.1804
16OH-RA peak 3
[M-H] 315 m/z
241.1957
271.2062
297.2428
253.1956
315.1956
18OH-RA peak 4
[M-H] 315 m/z
253.1957
271.2062
297.2429
241.1958
315.1957
Relative Abundance
m/z
time (minutes)
atRA-d5
4OH-RA, peak 1
[M-H] 319 m/z
257.2207
275.2312
319.2209
4oxo-RA peak 2
[M-H] 316 m/z
297.2428
272.2094
254.1678
16OH-RA peak 3
[M-H] 320 m/z
320.2274
246.2274
257.2211
276.2380
18OH-RA peak 4
[M-H] 319 m/z
319.2211
257.2210
275.2316
d5-atRA

Figure 3

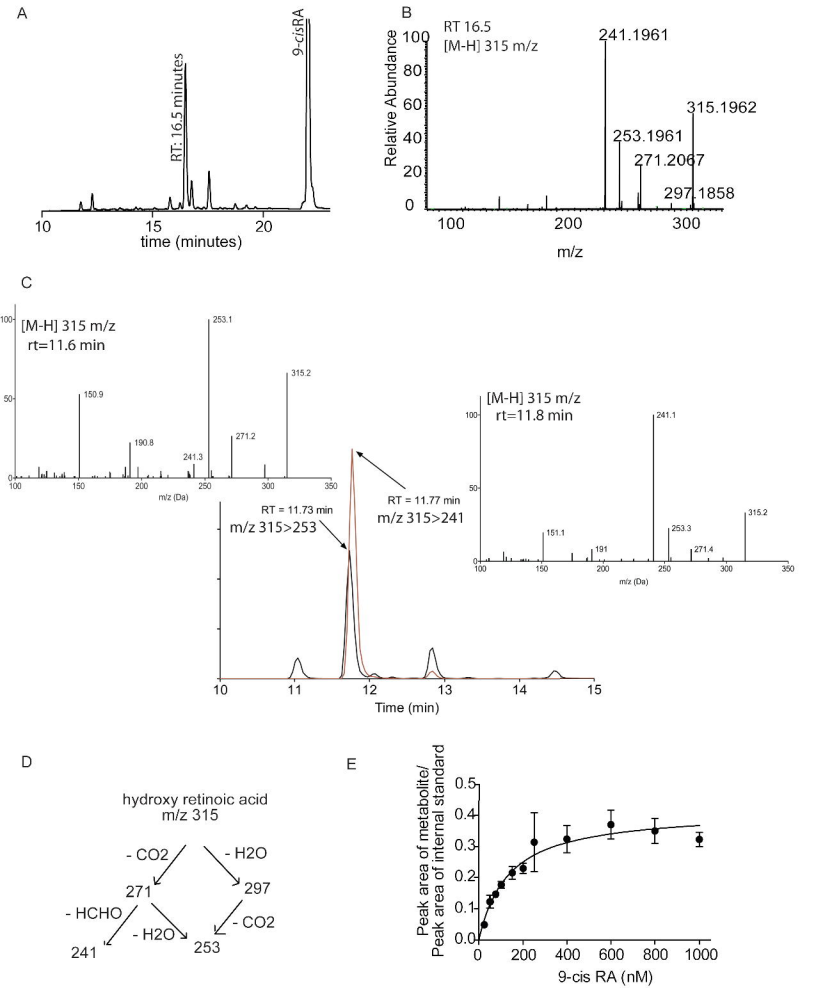
A
RT. 16.5 minutes
9-cisRA
time (minutes)
B
RT 16.5
[M-H] 315 m/z
Relative Abundance
241.1961
315.1962
253.1961
271.2067
297.1858
m/z
C
[M-H] 315 m/z
rt=11.6 min
[M-H] 315 m/z
rt=11.8 min
RT = 11.73 min
m/z 315>253
RT = 11.77 min
m/z 315>241
Time (min)
D
hydroxy retinoic acid
m/z 315
- CO2
- H2O
271
297
- HCHO
- H2O
- CO2
241
253
E
Peak area of metabolite/
Peak area of internal standard
9-cis RA (nM)

Figure 4

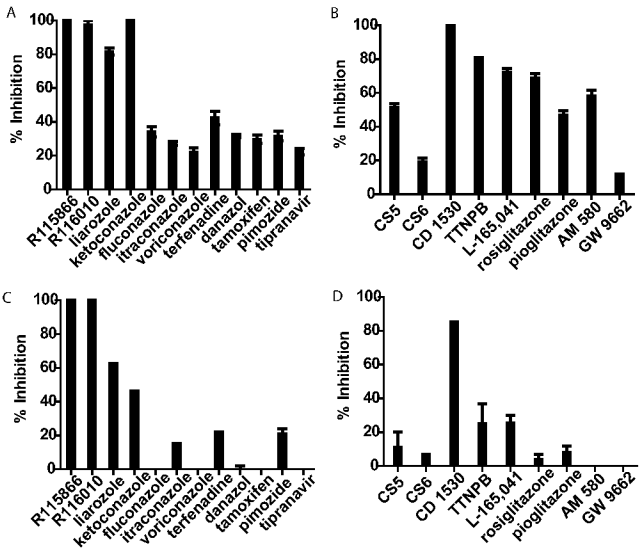
A
% Inhibition
100
80
60
40
20
0
R115866
R116010
ilarozole
ketoconazole
fluconazole
itraconazole
voriconazole
terfenadine
danazol
tamoxifen
pimozide
tipranavir
B
% Inhibition
CS5
CS6
CD 1530
TTNPB
L-165,041
rosiglitazone
pioglitazone
AM 580
GW 9662
C
% Inhibition
D
% Inhibition

Figure 5

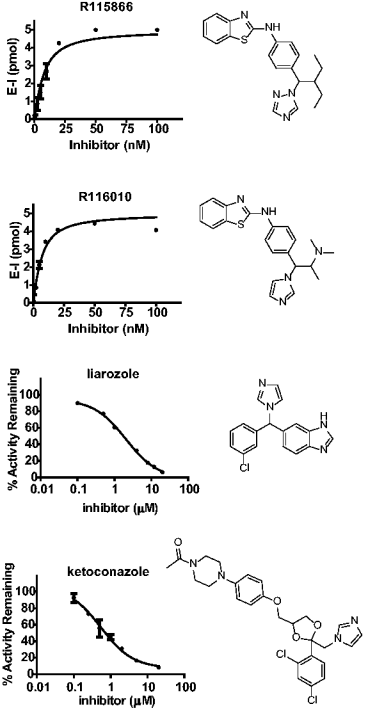
R115866
E-I (pmol)
Inhibitor (nM)
R116010
E-I (pmol)
Inhibitor (nM)
Ilarozole
% Activity Remaining
inhibitor (μM)
ketoconazole
% Activity Remaining
inhibitor (μM)

Figure 6

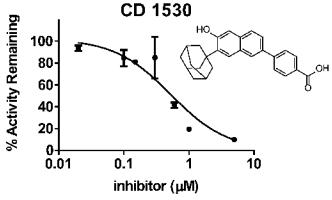
CD 1530
% Activity Remaining
inhibitor (μM)

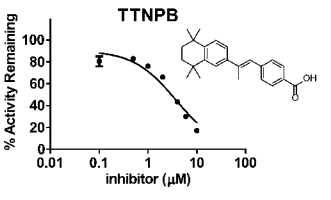
TTNPB
% Activity Remaining
inhibitor (μM)

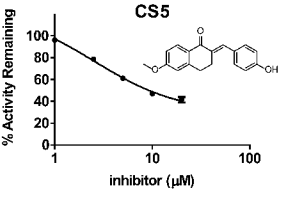
CS5
% Activity Remaining
inhibitor (μM)

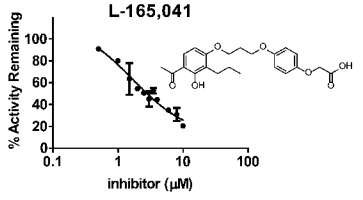
L-165,041
% Activity Remaining
inhibitor (μM)

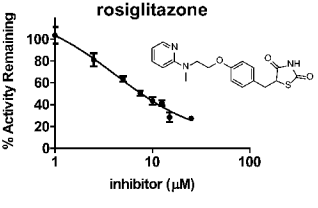
rosiglitazone
% Activity Remaining
inhibitor (μM)

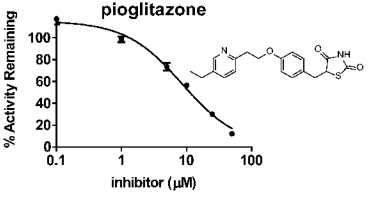
pioglitazone
% Activity Remaining
inhibitor (μM)

Figure 7

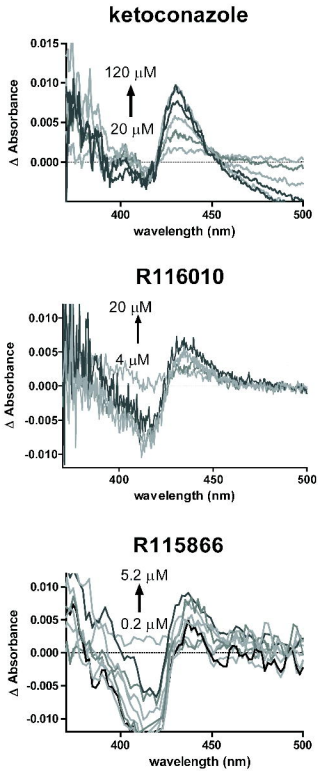
ketoconazole
0.015
0.010
0.005
0.000
120 μM
20 μM
Δ Absorbance
400
450
500
wavelength (nm)
R116010
20 μM
4 μM
0.010
0.005
0.000
-0.005
-0.010
Δ Absorbance
400
450
500
wavelength (nm)
R115866
5.2 μM
0.2 μM
0.010
0.005
0.000
-0.005
-0.010
Δ Absorbance
400
450
500
wavelength (nm)